EJNMMI Radiopharmacy and Chemistry

RESEARCH ARTICLE Open Access

Design and development of nanoprobes radiolabelled with ^{99m}Tc for the diagnosis and monitoring of therapeutic interventions in oncology preclinical research

María Jimena Salgueiro[1,2*], Mariano Portillo[1,2], Fiorella Tesán[1], Melisa Nicoud[3,4], Vanina Medina[3,4], Marcela Moretton[2,4,5], Diego Chiappetta[2,4,5] and Marcela Zubillaga[1,2,4]

*Correspondence:
María Jimena Salgueiro
jsalgueiro@ffyb.uba.ar
[1]Cátedra de Física, Facultad de Farmacia y Bioquímica, Universidad de Buenos Aires, Junín 956 PB , Buenos Aires (1113), Argentina
[2]Instituto de Tecnología Farmacéutica y Biofarmacia (InTecFyB), Universidad de Buenos Aires, Buenos Aires, Argentina
[3]Laboratory of Tumor Biology and Inflammation, Biomedical Research Institute (BIOMED), Faculty of Medical Sciences, Pontifical Catholic University of Argentina, (UCA-CONICET), Buenos Aires, Argentina
[4]Consejo Nacional de Investigaciones Científicas y Técnicas (CONICET), Buenos Aires, Argentina
[5]Cátedra de Tecnología Farmacéutica I, Facultad de Farmacia y Bioquímica, Universidad de Buenos Aires, Buenos Aires, Argentina

Abstract

Background Previous studies employing polymeric micelles and molecular imaging for in vivo nanosystem characterization have led to the development of radionanoprobes (RNPs) designed for diagnosing and monitoring therapeutic interventions in preclinical oncology research, specifically within breast and colon cancer models. These models exhibit high GLUT1 expression on tumor cells and VEGFR expression on the tumor vasculature. We aimed to enhance the tumor-targeting specificity of these RNPs by functionalizing micelles with glucose and bevacizumab. The choice of ^{99m}Tc to label the nanoprobes is based on its availability and that direct labeling method is a widespread strategy to prepare radiopharmaceuticals using cold reagents and a ^{99}Mo/^{99m}Tc generator. Soluplus® is an attractive polymer for synthesizing micelles that also allows their functionalization. With all the above, the objective of this work was to design, develop and characterize nanoprobes based on polymeric micelles and radiolabeled with ^{99m}Tc for the characterization of biological processes associated to the diagnosis, prognosis and monitoring of animal models of breast and colon cancer in preclinical research using molecular images.

Results Four RNPs ([^{99m}Tc]Tc-Soluplus®, [^{99m}Tc]Tc-Soluplus®+TPGS, [^{99m}Tc]Tc-Soluplus®+glucose and [^{99m}Tc]Tc-Soluplus®+bevacizumab) were produced with high radiochemical purity (> 95% in all cases) and stability in murine serum for up to 3 h. The RNPs maintained the 100 nm size of the Soluplus® polymeric micelles even when they were functionalized and labeled with ^{99m}Tc. The image acquisition protocol enabled the visualization of tumor uptake in two cancer experimental models using the assigned RNPs. In vivo biological characterization showed signal-to-background ratios of 1.7 ± 0.03 for [^{99m}Tc]Tc-Soluplus®+TPGS, 1.8 ± 0.02 for [^{99m}Tc]Tc-Soluplus®, and 2.3 ± 0.02 for [^{99m}Tc]Tc-Soluplus®+glucose in the breast cancer model, and 1.8 ± 0.04 for [^{99m}Tc]Tc-Soluplus® and 3.7 ± 0.07 for [^{99m}Tc]Tc-Soluplus®+bevacizumab in the colon cancer model. Ex vivo biodistribution, showed that the uptake of the tumors, regardless of the model, is < 2% IA/g while the blood activity concentration is higher,

© The Author(s) 2024. **Open Access** This article is licensed under a Creative Commons Attribution-NonCommercial-NoDerivatives 4.0 International License, which permits any non-commercial use, sharing, distribution and reproduction in any medium or format, as long as you give appropriate credit to the original author(s) and the source, provide a link to the Creative Commons licence, and indicate if you modified the licensed material. You do not have permission under this licence to share adapted material derived from this article or parts of it. The images or other third party material in this article are included in the article's Creative Commons licence, unless indicated otherwise in a credit line to the material. If material is not included in the article's Creative Commons licence and your intended use is not permitted by statutory regulation or exceeds the permitted use, you will need to obtain permission directly from the copyright holder. To view a copy of this licence, visit http://creativecommons.org/licenses/by-nc-nd/4.0/.

suggesting that the *enhanced permeability and retention* effect (EPR) would be one of the mechanisms involved in imaging tumors in addition to the active targeting of RNPs.

Conclusions Soluplus®-based polymeric micelles provide a promising nanotechnological platform for the development of RNPs. The functionalization with glucose and bevacizumab enhances tumor specificity enabling effective imaging and monitoring of cancer in animal models.

Keywords Micelles, ^{99m}Tc, Molecular imaging, Oncology

Introduction

The use of nanotechnology for diagnosis and monitoring biological systems is a growing area with great impact in health sciences. Particularly, its applications in therapeutic drug delivery and imaging techniques have gained great attention from the pharmaceutical and radiopharmaceutical community (Boerman et al. 2000; Torchilin 2007a; Torchilin 2007b). In this sense, of the numerous variants of nanoparticles available, liposomes and polymeric micelles are among the most investigated to improve the biological distribution pattern and increase the uptake of different compounds in target sites for both the diagnosis and treatment of infectious, inflammatory and tumoral processes (Dams et al. 1998; Bao et al. 2003; Camo et al. 2008; Pereira et al. 2009; Underwood et al. 2012). Thus, modifications have been made to the surface of the nanosystems with different agents (Sawant and Torchilin 2012; Alien and Cullies 2013; Riedel et al. 2022; Girón et al. 2024) in order to prolong their circulation in the blood and increase their ability to accumulate in solid tumors via the effect of enhanced permeability and retention known as EPR in the tumor vasculature (Maeda et al. 2000; Nichols and Bae 2014). In this case, there is a single precedent in the development of modified liposomes as a vehicle for [^{99m}Tc]Tc-sestamibi for the diagnosis of tumors with promising results (Belhaj-Tayeb et al. 2003). This strategy constitutes one of the possibilities for using radiolabeled nanoprobes, carrying classic radiopharmaceuticals such as [^{99m}Tc]Tc-sestamibi. The other is the labeling of nanosystems in order to obtain preclinical functional images for the diagnosis, monitoring and prognosis of oncological diseases. Based on everything described above, we focused on the search for nano systems with the potential to be radiolabeled for use as a diagnostic probe in preclinical oncology. One of the nanosystems we evaluated was d-α-tocopheryl polyethylene glycol succinate 1000 (TPGS) micelles with promising results which were published in a timely manner (Tesan et al. 2017).

The development of animal models for oncology studies remains a challenge, particularly in cases of breast and colon cancer because they constitute the highest incidence. According to the National Cancer Institute, breast cancer was the one with the highest incidence in 2020, representing 16.8% of all new cases and is the most frequently diagnosed in women. In second place is colorectal cancer, representing 12.1% of all tumors (INC 2020).

Our experience with polymeric micelles, molecular imaging for the in vivo study and characterization of nanosystems and the development of radiopharmaceuticals leads us to develop radionanoprobes (RNPs) to carry out the diagnosis and monitoring of interventions in preclinical research with animal models of breast and colon cancer. The choice to label with ^{99m}Tc is due to its availability and from the radiochemical point of view, a direct labeling technique analogous to the cold reagent kits. Soluplus® is an attractive polymer for synthesizing micelles that also allows their functionalization. In

this way, the target specificity would be improved in addition to the EPR effect of the nanoparticles.

In recent years Soluplus® stands as a promising biocompatible copolymer to develop different nanoformulations based in polymeric micelles. These nanocarriers are dynamic systems composed by amphiphilic polymers that self-assemble into polymeric micelles upon their critical micellar concentration (CMC) in water. Thereby, polymeric micelles present a hydrophobic core which is able to host poorly-water soluble drugs and a hydrophilic corona which provides colloidal stability to the nanocarrier (Owen et al. 2012).

Particularly, Soluplus® is a graft copolymer of poly (vinyl caprolactam)-poly (vinyl acetate)-poly (ethylene glycol) (PEG) with excellent solubilizing properties of hydrophobic drugs along with high colloidal stability mainly associated with its low CMC value. Moreover, micellar nanoformulations based in Soluplus® has been successfully developed over the last decade. For instance, respirable Soluplus® micelles have been investigated for rifampicin and rifampicin/curcumin pulmonary delivery (Galdoporpora et al. 2022; Grotz et al. 2019) to improve tuberculosis pharmacotherapy. Further, effective inhalable Soluplus® micelles loaded with voriconazole has been studied as a promising strategy for fungal infections in cystic fibrosis patients (Briceño Fernandez et al. 2024). Also, this strategy was explored to develop oral micellar dispersions to improve biopharmaceutical efavirenz properties (Fuentes et al. 2024). Other Soluplus® involved the encapsulation of hydrophobic drugs as carvedilol (Wegmann et al. 2017), doxorubicin (Jin et al. 2015), quercetin (Dian et al. 2014), paclitaxel and histamine (Maravajjala et al. 2020; Nicoud et al. 2023). Furthermore, mixed micelles of Soluplus® and other amphiphilic polymers were studied to enhance breast and ovarian cancer chemotherapy (Moretton et al. 2017; Riedel et al. 2021).

Modification of the micelles with gluconolactone (glucose) is rooted in the unique metabolic characteristics of cancer cells, particularly their increased glucose uptake, which is mediated by the overexpression of glucose transporter proteins (GLUTs 1–14). Among these, GLUT1 is notably overexpressed in breast cancer tissues and is associated with metastasis. This overexpression suggests that GLUT1 could serve as an effective target for drug delivery to breast tumor tissues. Consequently, the modification of micelles with glucose residues aims to leverage this characteristic for targeted delivery to cancer cells (Moretton 2017).

Bevacizumab, an FDA-approved monoclonal antibody, targets Vascular Endothelial Growth Factor (VEGF) and effectively inhibits angiogenesis, a critical process in tumor growth and metastasis. Functionalizing drug delivery systems with bevacizumab offers the potential to enhance tumor targeting, not only through the passive Enhanced Permeability and Retention (EPR) effect but also by actively targeting VEGFR-expressing tumor vasculature. In this study, we hypothesized that the functionalization of Soluplus® micelles with bevacizumab would improve tumor localization by combining passive accumulation with active targeting mechanisms. Although the use of bevacizumab-functionalized nanocarriers has been explored in other systems (Tesan et al. 2016), this represents one of the first studies investigating the functionalization of Soluplus® micelles with bevacizumab for enhanced tumor targeting.

With all the above, the objective of this work was to design, develop and characterize nanoprobes based on polymeric micelles radiolabeled with ^{99m}Tc for the characterization of biological processes linked to the diagnosis, prognosis and monitoring of breast

and colon cancer animal models for preclinical research using molecular images and set up imaging protocols in experimental animals, contributing to the concept of the 3Rs and optimizing the experimental protocols in which they are used.

Materials and methods

The experimental design of the work is schematized in Fig. 1.

Materials

Radioactive

^{99}Mo/^{99m}Tc-generator (Laboratorios Bacon SAIC, Argentina) was employed to obtain the sterile-non-pyrogenic sodium pertechnetate solution ([^{99m}Tc]$NaTcO_4$) which was used in the labeling of the RNPs.

Nanotechnology platforms

Soluplus® is an amphiphilic graft copolymer composed of a polyvinyl caprolactam, polyvinyl acetate and polyethylene glycol 6000 (Soluplus®) developed by BASF and first introduced in October 2009 (Djuric and Hardung 2009). It exhibits an average molecular weight ranging between 90,000 and 140,000 g/mol (Hardung et al. 2010).

Nanoprobe functionalizing materials: TPGS, glucose and Bevacizumab

TPGS, also known as vitamin E TPGS, is a biocompatible compound that has been approved by the FDA. It possesses the unique ability to form nanometric micelles in aqueous solutions.

Glucose in the form of ɣ-gluconolactone serves as a precursor for the glycosylation of Soluplus® polymeric micelles. This glycosylation occurs through a ring-opening reaction, facilitated by microwave radiation, contributing to the functionalization of the micelles.

Bevacizumab, commercially known as Avastin®, is an FDA-approved monoclonal antibody targeting VEGF. It plays a crucial role in inhibiting angiogenesis, which is vital for

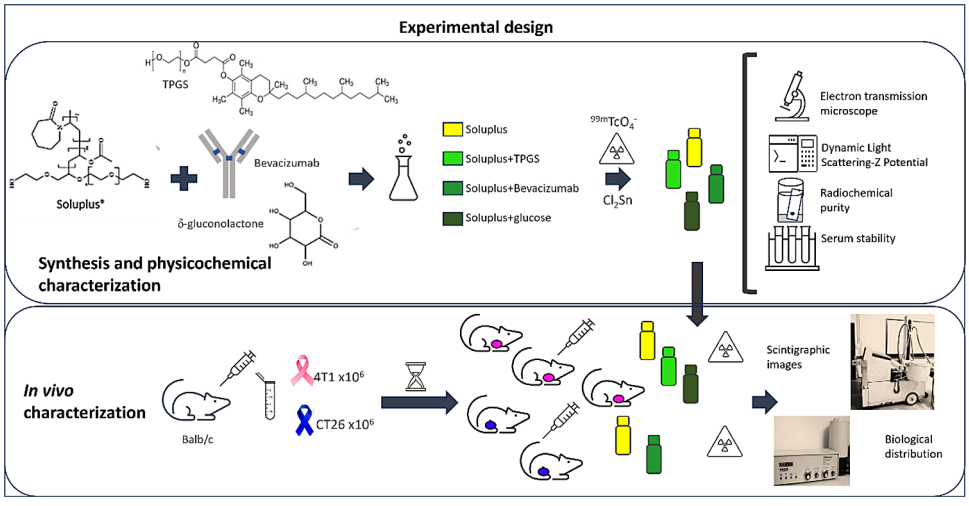

Fig. 1 Scheme of the experimental design. The above panel outlines the synthesis, labeling and physicochemical characterization of the RNPs using radiochemical purity tests, stability in murine serum, dynamic light scattering and electron microscopy. The panel below shows the scheme used for the in vivo characterization of the RNPs using planar scintigraphy and subsequent ex vivo biological distribution in two experimental cancer models: breast and colon

the growth of tumors. Bevacizumab is commonly used in the treatment of several cancers, particularly metastatic types such as metastatic colorectal cancer and non-small cell lung cancer.

Quality control of intermediate and final RNPs preparations

The pH of the preparations is measured using Merck test strips (pH 1–10, Merck, Germany). The activity of the preparations is determined in a calibrated ionization chamber, with results expressed in megabecquerels (MBq) (Vexcal, Argentina). To confirm radionuclide purity, the samples were placed in 6 mm lead shields and measured in an ionization chamber, following the protocol outlined in the 7th Edition of the Argentine Pharmacopoeia (2013).

Radiochemical purity was assessed through Instant Thin Layer Chromatography (ITLC) as stationary phase (Variant, Argentina), while mobile phases include Acetone, and a mixture of pyridine, acetic acid, and distilled water in a 5:3:1.5 ratio, as documented in the literature (Psimadas et al. 2014).

When acetone is used as the mobile phase, free pertechnetate migrates with an Rf value of 1, allowing it to be separated from all labeled species, which remain at Rf: 0. In contrast, when using the pyridine mixture as the mobile phase, large radiocolloids stay at Rf: 0, while all other radioactive species migrate to Rf values between 0.8 and 1.

Animals

BALB/c mice were used as animal models, obtained from authorized vivariums (Central Bioterio, School of Pharmacy and Biochemistry, University of Buenos Aires, Argentina). The animals were housed in ventilated cabinets (Animal Fresh Air, Argentina), grouped 5–6 per cage with ad libitum access to water and balanced mouse food (GANAVE, Argentina). Environmental conditions were maintained at 22–23 °C with a humidity of approximately 56% and 12-hour light-dark cycles. All animal care and use were conducted in accordance with the Guide for the Care and Use of Laboratory Animals, 8th Edition (2011). For scintigraphic studies, anesthesia was induced by inhalation of 2% v/v isoflurane (Scott-Casará, Argentina) administered via a mask connected to a vaporization system with oxygen entrainment (Forane, Ohio Medical Products). Euthanasia for ex vivo biological distribution tests was performed using a CO_2 chamber.

The protocols were approved by the Institutional Commission for the Care and Use of Laboratory Animals (CICUAL; Res (D) N°671/18) at the School of Pharmacy and Biochemistry, University of Buenos Aires.

Cell lines

The 4T1 cell line (ATCC CRL-2539) is a murine tumor cell line derived from the BALB/cfC3H mouse strain. It is resistant to 6-thioguanine and serves as a model for studying stage IV human breast cancer. This cell line is highly tumorigenic and can induce tumors with the ability to metastasize to the lungs, liver, lymph nodes, and brain in BALB/c mice (ATCC 2024a).

The CT26WT cell line (ATCC CRL-2638), is an undifferentiated colon carcinoma cell line. It was originally induced by the carcinogen N-nitroso-N-methylurethane (NNMU) and later cloned to establish this widely used line (ATCC 2024b).

Methods

Preparation of radionanoprobes

Soluplus® micelles (10% w/v) were prepared by dissolving the appropriate amount of polymer in distilled water under magnetic stirring (50 rpm) at 25 °C. The samples were then equilibrated at room temperature for 24 h before use. Functionalized micelles were prepared following three different procedures, as described below.

To prepare functionalized micelles, a final concentration of 10% w/v and a Soluplus®:TPGS ratio of 5:1 were used. Specifically, 830 mg of Soluplus® and 170 mg of TPGS were dispersed in 10 mL of distilled water.

Micelles containing bevacizumab were prepared by adding 800 µL of a 25 mg/ mL bevacizumab (Avastin®) solution to the previous dispersion, resulting in a final antibody concentration of 2 mg/ mL. For the physicochemical characterization, a control antibody sample of the same concentration was prepared for comparison purposes.

The conjugation of Soluplus® with glucose was carried out via a ring-opening reaction of ɣ- gluconolactone in the presence of the –OH terminal of PEG. This reaction was assisted by microwave radiation, following the method previously reported by Taich et al. (2016) and Moretton et al. (2015). In brief, 5 g of Soluplus® copolymer were dissolved in 10 mL of dimethylformamide (DMF), along with 42.7 mg of ɣ-gluconolactone, under magnetic stirring at 100 rpm. The reaction mixture was placed in a 250 mL flask and dried under vacuum for 3 h in a glycerin bath maintained at 100–110 °C. Then, 13.5 µL of tin octanoate [$Sn(Oct)_2$] was added as a catalyst (in a 1:1 molar ratio with Soluplus®). The flask was then placed in a microwave oven (Whirlpool, WMD20SB, microwave frequency 2450 MHz, power 800 W, Argentina) equipped with a laboratory-adapted capacitor. The reaction mixture was subjected to microwave radiation for 1 min at power level 2, followed by 14 additional minutes at power level 1, resulting in a total reaction time of 15 min. Following the reaction, the mixture was diluted with 10 mL of distilled water and dialyzed (Spectra/Por dialysis membrane, molecular weight cutoff=3500 Da, nominal width 45 mm, USA) against distilled water for 3 days. Finally, the Soluplus®-glucose nanoprobe was recovered in distilled water and stored for subsequent characterization.

Labeling and physicochemical characterization

The radiolabeling of Soluplus® micelles and their functionalized counterparts was performed using a direct labeling approach. Several methodologies were tested (data not shown), and the radiolabeling process using $SnCl_2$ was selected as the most effective method for achieving successful labeling. Preformed micelles were prepared at a concentration of 10% w/v in distilled water. To this solution, 25 µg of $SnCl_2$ (from a 1 mg/mL solution acidified with HCl) was added. Subsequently, 200–300 µL of a [^{99m}Tc]$NaTcO_4$ solution, with an activity of approximately 55.5 MBq, was added to the reaction vial. The pH was then adjusted to 6 using 0.1 N NaOH. The reaction mixture was incubated at room temperature for 30 min, after which the physicochemical characterization of the RNP systems was conducted. Radiochemical purity was assessed using two distinct chromatographic systems, both employing ITLC as the stationary phase. In one system, acetone was used as the mobile phase to separate free [^{99m}Tc]$NaTcO_4$. In the other, a mobile phase consisting of pyridine, acetic acid, and water (5:3:1.5 ratio) was employed. The stability of the radiolabeled nanoprobes was evaluated by incubating an aliquot of each system (25 µL) at 37 °C with 250 µL of freshly obtained mouse serum. At 0.5, 1,

2, and 3 h of incubation, 5 μL aliquots were withdrawn, and the radiochemical purity was determined. The average hydrodynamic size and size distribution of the micelles were determined by dynamic light scattering (Zetasizer Nano-Zs, Malvern Instruments, UK) with a He-Ne laser (633 nm) and a ZEN3600 digital correlator. The measurements were carried out at an angle of θ = 173° with relative to the incident beam, previously equilibrating the samples at 25 °C for 5 min. The Z potential was measured using the same equipment. All measurements were performed in triplicate, and the results were reported as the average of the three measurements. The morphology of the micelles was analyzed using transmission electron microscopy (TEM) on a Zeiss EM 109T equipped with a Gatan ES1000W digital camera. This analysis was conducted at the Electron Microscopy Service of LANAIS-MIE, part of the National Microscopy Service. For TEM sample preparation, aliquots of the micelle suspension were placed on a grid covered with Formvar film. The samples were then stained with 5 μL of phosphotungstic acid (1% w/v), washed with distilled water, and dried in a silica gel container before imaging.

Generation of tumor models

Mammary 4T1 (ATCC CRL-2539) and colon CT26WT (ATCC CRL-2638) tumor cells were cultured in Roswell Park Memorial Institute (RPMI) 1640 medium (Gibco, Life Technologies Corporation, USA) supplemented with 10% fetal bovine serum (FBS, Gibco, Life Technologies Corporation, USA), glutamine (Gibco, Life Technologies Corporation, USA) at 0.03% and penicillin-streptomycin (Sigma Aldrich, USA) at 0.001% (complete medium). The cells were maintained in a culture oven at 37 °C in a humidified atmosphere with 5% CO_2 were subcultured 2–3 times a week, for which the culture medium was aspirated, the monolayer was washed with physiological solution (0.9% NaCl solution) and harvested with a trypsin/EDTA solution (0.25%, ethylenediaminetetraacetic acid (EDTA) 1 mM).

The murine breast cancer model was induced in immunocompetent female mice ($n = 9$) between 6 and 8 weeks old, of the BALB-c strain (weight: 25–30 g) by injecting 10^6 cells subcutaneously and orthotopically into the superior's mammary glands. The murine colon cancer model was induced in immunocompetent male mice ($n = 6$) between 6 and 8 weeks old, of the BALB-c strain (weight: 25–30 g) by injecting 10^6 murine cells subcutaneously in the rear flank. For both models, the evolution of tumor size was measured daily using a caliper after implantation.

Planar scintigraphy in animal models

RNP administration was performed via intravenous injection through the lateral tail vein of the mice ($n = 3$ per group). Imaging acquisition was conducted 1 h after the biological distribution phase using a small-field planar gamma camera (OHIO NUCLEAR, Argentina). The gamma camera was equipped with a high-sensitivity collimator and operated with data and image processing software specifically adapted for small animal studies (Version 3.4, IM512P, Alfanuclear, Argentina). Images were acquired in static mode using a matrix of 256×256 pixels, with zoom adjustments made according to the size of the animal. To minimize measurement errors to less than 1%, the collected counts were carefully related to the counting statistics. For image analysis, the acquired images were displayed using Neat A scale for the breast cancer model and Neat B scale for the colon cancer model. Regions of interest (ROIs) corresponding to the uptake of the RNP

in various organs were delineated on the images. Signal-to-background ratios were calculated for these ROIs to assess the distribution of the RNP. Results were expressed as means ± SD and were correlated with data obtained from ex vivo experiments to ensure consistency and accuracy of the findings.

Biodistribution studies in animal models

The biological distribution observed in planar scintigraphy images, the activity of the administration syringe was measured using a dose calibrator (Vexcal, Argentina) both before and after injection. The net injected activity was determined by calculating the difference between these measurements. During the biodistribution period (1 h), the animals were housed in their cages within a vivarium sector equipped with lead shielding to minimize work radiation exposure. After the biodistribution period, the animals were euthanized, and the organs of interest were excised. Each organ was weighed and subsequently measured using a calibrated solid scintillation counter (Alfanuclear, Argentina). The results were expressed as a percentage of the injected activity per gram of tissue (% IA/g) and were normalized by the tissue mass. Additionally, tumor-to-blood uptake ratios were calculated.

Data analysis and statistics

All statistical analyses were conducted using GraphPad Prism 6 (GraphPad Software, Inc.). For the evaluation of biodistribution results in the breast cancer model, data were analyzed using a one-way ANOVA test followed by a Tukey post- test to determine pairwise comparisons. The biodistribution results for the colon cancer model were assessed using an unpaired Student's t-test. Statistical significance was defined as a p-value of less than 0.05.

Results

The results demonstrate that the RNP based on Soluplus® micelles has a size of 100 nm with an approximately spherical shape and neutral Z potential (mV (+/-DE) = -0.3 (0.1)) (Fig. 2). The functionalization, or decoration, of the Soluplus® micelles with TPGS, glucose or bevacizumab to generate the active orientation did not modify the original size in the different derived RNPs (Fig. 2) which, in turn, preserved neutral Z potential. This means that the size distribution of the micelles with and without decoration that make up the RNPs, characterized in terms of DLS at 25 °C, demonstrated in all cases unimodal behavior with hydrodynamic diameter values of around 100 nm, which were maintained after labeling with ^{99m}Tc, a fact indicative of adequate stability during the processes carried out. Additionally, the DLS of bevacizumab and that of TPGS allow us to compare the sizes of these functionalizing materials individually with respect to when they are part of the RNP as a control for incorporation into the RNPs.

The radiochemical purity test showed results greater than 95% for all RNPs. This means that not only was a high labeling efficiency achieved by incorporating ^{99m}Tc into the RNP, demonstrated using the chromatographic system integrated by ITLC and acetone, but that the formation of colloidal species derived from the reduced and hydrolyzed ^{99m}Tc was very low as was demonstrated using the ITLC system with the pyridine mixture as the mobile phase. The DLS control of the [^{99m}Tc]Tc-colloidal (simulated by identical preparation of the RNPs except for the addition of Soluplus®) is also a marker

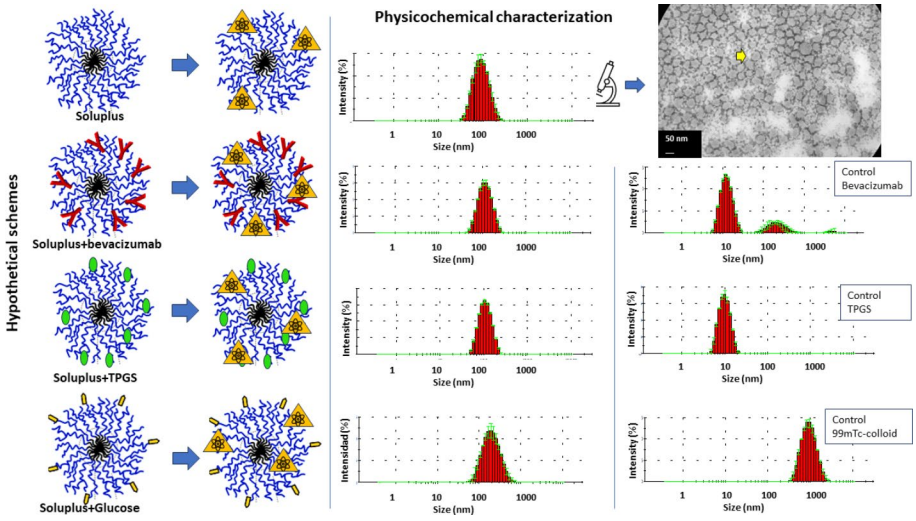

Fig. 2 Results of the physicochemical characterization of the RNPs. The left panel shows the scheme of the RNPs made up of Soluplus® and its functionalizing materials (bevacizumab, TPGS and glucose) and the labeling with ^{99m}Tc. The right panel shows the results of the DLS measurements of the hydrodynamic diameter of the RNPs, in which the presence of only one peak can be observed, indicating the unimodal behavior of the preparation, (right) DLS measurements of the hydrodynamic diameter of the functionalizers and [^{99m}Tc]Tc-colloid for comparative purposes, discarding impurities of functionalizers without incorporating into the RNP and the absence of [^{99m}Tc]Tc-colloidal in the preparations. The photo (upper right) corresponds to the electron microscopy performed on the RNP made of Soluplus® in which the spherical shape of the 100 nm micelles can be observed (yellow arrow)

of radiochemical purity and reinforces the result obtained by the chromatographic technique given that the DLS of each of the RNPs the peak corresponding to [^{99m}Tc]Tc-colloidal is not observed (Fig. 2). Therefore, the observed biological distribution can be attributed to the biological behavior of RNPs as particulate systems, without interference that could arise from the presence of colloidal impurities that are commonly generated in labeling in which stannous chloride is used as a reducing agent. On the other hand, the stability of radiochemical purity in vivo was simulated by incubation of the RNPs in murine serum at 37 °C and the results showed values greater than 92% up to 3 h of incubation.

In relation to the biological characterization of the RNPs, Fig. 3 shows two panels containing representative images of each RNP used in the experimental models of breast cancer (top) and colon cancer (bottom) accompanied by the. ex vivo biological distribution results.

All the designed RNPs allowed the visualization of tumors in both experimental cancer models in the configuration developed for the image acquisition protocol (Fig. 1). The in vivo behavior of the RNPs according to their physicochemical characteristics could be studied and analyzed in the acquired planar images and the results were validated by ex vivo biological distribution assays.

In the experimental breast cancer model, the images show a similar biological distribution pattern for the Soluplus® RNP and for those functionalized with both TPGS and glucose. After 1 h of administration, the Soluplus® RNP shows permanence in blood circulation, hepatic and splenic uptake attributable to its condition as a micellar system whose pharmacokinetics would reveal phenomena of phagocytosis and opsonization, and renal uptake indicating an excretion mechanism through of urine. The tumor, palpable upon clinical examination of the experimental animal as part of the monitoring, is

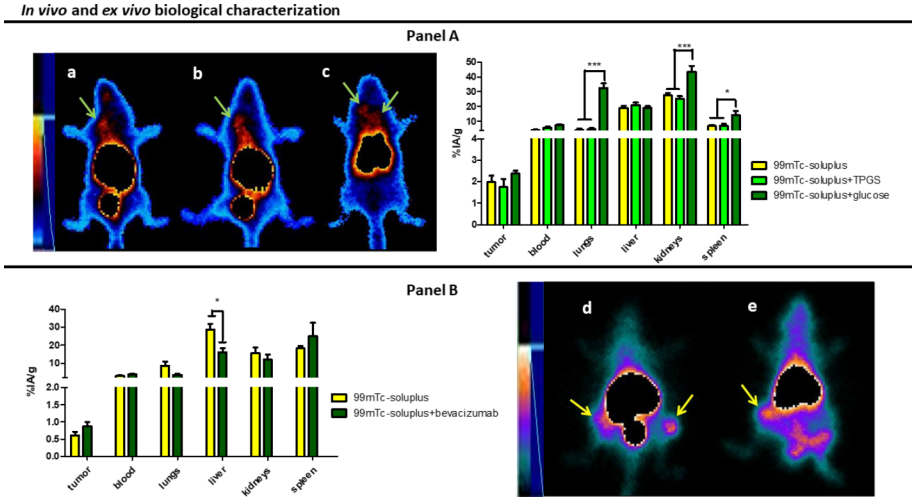

Fig. 3 Panel **A** (upper): (left) scintigraphic images representative of the biodistribution of RNPs; a) [^{99m}Tc]Tc-Soluplus®, b) [^{99m}Tc]Tc-Soluplus®+TPGS, (c) [^{99m}Tc]Tc-Soluplus®+glucose. All three RNPs allow tumor visualization (arrows). Color scale was adjusted to remove the high liver, kidney and bladder uptake to more clearly visualize the tumor. (right) ex vivo biodistribution results expressed as % ID/g; [^{99m}Tc]Tc-Soluplus®+glucose showed increased uptake in liver, lungs and spleen (*$p < 0{,}05$; ***$p < 0{,}01$). Panel **B** (bottom): (left) ex vivo biodistribution results expressed as % IA/g; [^{99m}Tc]Tc-Soluplus® showed increased uptake in liver, (*$p < 0{,}05$). (right) scintigraphic images representative of the biodistribution of RNPs; (d) [^{99m}Tc]Tc-Soluplus®, (e) [^{99m}Tc]Tc-Soluplus®+bevacizumab. The two RNPs allow tumor visualization (arrows). Color scale was adjusted in the two panels to remove the high liver, kidney and bladder uptake to more clearly visualize the tumor

Table 1 RNP uptake ratio in experimental tumor models obtained in the biological characterization carried out by in vivo scintigraphic images and ex vivo biological distribution

	In vivo Tumor/background	Ex vivo Tumor/blood
Model Balb/c + 4T1 breast cancer		
[^{99m}Tc]Tc-Soluplus®	1.8 ± 0.02	0.5 ± 0.02
[^{99m}Tc]Tc-Soluplus® +TPGS	1.7 ± 0.03	0.3 ± 0.01
[^{99m}Tc]Tc-Soluplus® +glucose	2.3 ± 0.02*	0.3 ± 0.005
Model Balb/c + CT26WT colon cancer		
[^{99m}Tc]Tc- Soluplus®	1.8 ± 0.04	0.2 ± 0.01
[^{99m}Tc]Tc-Soluplus® +bevacizumab	3.7 ± 0.07*	0.2 ± 0.01

* Statistically significant ($p < 0.05$)

clearly visualized in the image, probably due to the conjunction of several factors such as the persistence of the micellar system in circulation, the EPR effect, the selection of the generation site of the orthotopic tumor in the model and the design of the image acquisition protocol. The comparative analysis of the in vivo and ex vivo methodologies used for the biological characterization of the RNP (Table 1) highlights in a semiquantitative way the results observed in the qualitative analysis of the distribution of activity in the images versus the uptake of the tissues of interest expressed as percentage of administered activity normalized by tissue mass. In this way, the value of molecular imaging in the biological characterization of nanomaterials, provides insights into biological phenomena that cannot be fully assessed through in vitro or ex vivo methodologies. The permanence in circulation of the RNP demonstrated ex vivo supports the visualization of the tumor *in vivo* due to the EPR effect that allows the migration of the particles to

the tumor environment providing the appropriate signal/background ratio for tumor localization.

The decoration of the Soluplus® RNP with TPGS, with the aim of functionalizing the system to achieve its anatomic targeting, produces a biological distribution very similar to that described.

Soluplus® system decorated with glucose also allows visualization of the breast tumor developed in the animal model (Fig. 3). However, the semiquantitative analysis of the images for this result shows that the uptake occurs with an increased signal/background ratio compared to the passive system (Table 1).

In the colon cancer model the results were similar to those observed for the breast model. In principle, the images show a similar biological distribution pattern for the Soluplus® RNP and for the one functionalized with bevacizumab. After 1 h of administration, both show permanence in blood circulation, hepatic and splenic uptake and renal uptake, which, as already mentioned, are attributable to their condition as micellar systems subjected to phagocytosis and opsonization phenomena and to a lesser extent excreted through of the kidney in the urine. In all cases, the tumors, palpable during clinical examination, were clearly visualized in the scintigraphic images due to coincident factors such as the persistence of RNPs in circulation, the EPR effect, the selection of the site of tumor generation, which although in this case is heterotopic, presents minimal anatomical interferences and the design of the image acquisition protocol. On the other hand, the comparative analysis of the in vivo and *ex vivo methodologies* (Table 1) also suggests that other phenomena in addition to the EPR participate in the visualization of the tumor when using [^{99m}Tc]Tc-Soluplus® +bevacizumab. In this sense, functionalization with the monoclonal antibody bevacizumab increases the anchoring of the micelles in the tumor environment to an important degree to significantly increase the signal/background ratio achieved by the passive orientation of the RNP. [^{99m}Tc]Tc-Soluplus® for EPR effect through active targeting provided by decoration with bevacizumab.

Discussion

The work presented here focuses on the development of new RNPs labeled with ^{99m}Tc, for preclinical research in oncology. Particularly, interest in the study of nanoparticles as a platform for the development of molecular probes arose a few years ago from the use of liposomes (Belhaj-Tayeb et al. 2003). Here, we aimed on the use of polymeric micelles obtained from the use of amphiphilic copolymers. The main reason why amphiphilic copolymers are considered attractive biomaterials is related to their unique properties such as their hydrophilic/hydrophobic balance, molecular weight, and the possibility of functionalization. They can self-assemble in solution into more complex structures with a wide variety of morphologies such as spherical, vesicular, rod-shaped, and lamellar. Therefore, these biomaterials can be used for different applications, including drug delivery and diagnostic imaging, among others (Wang and Grayson 2012). Due to the chemical properties of each moiety, amphiphilic copolymers can be decorated with a wide variety of ligands to obtain drug carriers for active targeting or commonly referred to as "active targeting" (Deshmukh et al. 2017; Torchilin 2005). In this work, we can verify that the preparation processes of the RNPs resulted from simple and complete micellization followed by direct method labeling, similar to that used with cold reagent kits in conventional nuclear medicine, in which ^{99m}Tc is coupled to the RNPs (Fig. 2).

Performing images in animal models involves a great challenge given that there are no specific protocols, arising from the consensus of professionals dedicated to the practice. The selection of the type of study, as well as the configuration parameters of its acquisition, must be specially considered and each decision made must be analyzed in relation to the research hypothesis.As can be seen from the description in the experimental design, our equipment does not belong to the group of those dedicated to working on experimental animals, as it is a planar gamma camera with a reduced field of view, formerly used in clinical practice. There are numerous limitations to performing molecular imaging with such equipment, especially in relation to the spatial resolution of the images and the impossibility of performing tomographic acquisitions. However, the adaptation of the experimental designs as well as the fine-tuning of the image acquisition protocols allow us to use this equipment in the research. That is why the understanding of the observed biological distribution corresponds directly to the experience arising from the researchers' previous learning curve, the study of the physiology and anatomy of the animal model and the strategies of the specific experimental design. Among the strategies to resolve the superposition of structures we can mention the selection of the type of positioning of the specimen and its correct execution, the acquisition of images in different incidences and the use of markers. During positioning, it is essential to consider appropriately accommodating the animal on the acquisition bed in a symmetrical and centered manner and achieving stretching of the body, which is relaxed due to anesthesia, for a better distribution of the internal structures. Cold or hot markers usually assist in the interpretation of images from confirming the correct identification of the animal's flanks and delineating contours to interpreting the location of organs and lesions. In line with this, the experimental design strategy is key, and, in our case, it begins with the same selection of the tumor cell inoculation site to obtain the cancer model. That is why, depending on whether it is an orthotopic model or not, the consideration of the anatomical interference in the planar image guides us to the selection of the upper mammary chain in the breast cancer model to carry out tumor implantation. On the other hand, inoculation in areas of little anatomical interference is also preferred for monitoring tumor growth by palpation and measurement, as well as for some interventions and such was the case of the selection of the rear flank for the colon cancer model, also making the correlation with the image capture easier.

During the last decade, glycosylated biopolymers (also known as glycopolymers) have proven to be very attractive biomaterials given the possibility of actively transporting drugs and genes to certain organs and/or tissues through specific ligand-receptor mediated interactions (Song et al. 2012; Kizjakina et al. 2012; Wang et al. 2013). In this context, when talking about antineoplastic therapy, research has focused on the development of new nanotechnological platforms for the transport of drugs where the nanocarrier is "decorated" on its surface with ligands capable of interacting specifically with those receptors that are overexpressed in tumors (Ying et al. 2010; Li et al. 2011; Niu et al. 2014). Among these receptors is the superfamily of GLUT 1–14 transmembrane receptors, which participate in the transport of carbon compounds such as monosaccharides in almost all human cells (Mueckler and Thorens 2013); glucose being its main biological substrate (Niu et al. 2014; Mueckler and Thorens 2013). However, it has been reported that GLUT-type receptors are overexpressed in different solid tumors, especially due to the high glucose requirements of tumor tissues compared to normal tissues

(Szablewski 2013). This allows GLUT receptors to be positioned as potential targets for the active transport of antineoplastic drugs using nanotechnology. Breast cancer cells overexpress GLUT 1 (Medina and Owen 2002; Ganapathy et al. 2009), therefore the conjugation of a biopolymer with glucose is an interesting strategy to allow the development of potential nanoformulations capable of actively transporting antineoplastic drugs to the cells. tumors, thus optimizing breast cancer chemotherapy. In summary, the results suggest that other phenomena additional to the EPR cooperate to increase the tumor presence of the RNP in the image and in this sense, our result agrees with what has been reported in the literature given that, for the active uptake by functionalization of nanoparticles, in this case RNPs, the phenomenon occurs depending on the EPR effect to access the tumor space through the fenestrations of the blood vessels, the size and surface chemistry intervene in the degree of navigation through the tumor interstitial that is achieved, and functionalization is used as a strategy to increase the accumulation and anchor the RNPs to the cells, preventing their elimination by the liver or spleen or excreted through the kidney (Albanese et al. 2012). These results are supported by those obtained in the *ex vivo test*, which also show that this RNP has a slightly different distribution compared to those previously described given that the uptake in the lung is somewhat greater. The selected representative image shows that the increased lung uptake of [^{99m}Tc]Tc-Soluplus®+glucose does not prevent the visualization of the tumor even when its location is more medial as in the case of this individual. At this point it is worth remembering that, after the administration intravenous nanoparticles and molecules of size nanometric they enter in the system vascular to distribute to the organs and fabrics peripherals of the body, but inside of this compartment vascular find cells blood, platelets, factors of coagulation, and proteins plasma that, depending of the size and charge of the nanoparticles can suffer adsorption or opsonization by proteins serum. This phenomenon, in addition of improve the recognition of particles by the host immune system, alters the effective size of the particle and gives as result a particle diameter called hydrodynamic diameter in vivo, that can be considerably higher than the diameter in vitro of the nanoparticle. In previously published work by our group (Tesan et al. 2018), we also documented that body temperature may be a factor contributing to the increase in size due to agglomeration. Therefore, although for this RNP the lung uptake is slightly greater compared to its non- functionalized analogue, a condition that could be explained by the above, this does not affect its ability to reveal in the scintigraphic images the tumors developed in the animal model, a function that also achieves with a higher signal/background ratio, improving visualization and contrast with adjacent structures such as the lung (Longmire et al. 2008).

In relation to the comparisons of the biological distribution between both models, we can observe that the phenomena of hepatic and splenic uptake of particles occur in both cases, as well as the renal elimination of a certain percentage of the administered RNPs due to tubular secretion (Zhu et al. 2022; Mosleh-Shirazi 2021, Psimadas et al. 2013). No test has been carried out to study how the surface chemistry of RNPs can be affected in circulation and result in the generation of micellar coronas that differentiate their behavior in vivo. However, it is clear from the results obtained that although the micellar systems were constituted with the same base polymer, the decorations influenced the conformation of the surface corona which determined the strength of the interaction of the RNPs with the environment, modifying its biological distribution (Albanese et al.

2012). Comparable results with other RNPs in renal excretion were obtained by Ramos-Membrive (2021), Seo (2015) and Arranja (2016). The increased pulmonary uptake of [^{99m}Tc]Tc-Soluplus®+glucose is consistent with the findings of Psimadas et al. (2013) and Seo et al. (2015), who reported that RNPs can accumulate in the lungs, which, like other reticuloendothelial organs, can sequester nanoparticles.

The primary goal of this study was to develop RNPs for in vivo tumor imaging, rather than evaluating Soluplus® as a micellar delivery system. Within this framework, the results are promising, as they demonstrate the potential of the RNPs for effective tumor visualization. Although high uptake in the liver, spleen, and kidneys was observed, this does not interfere with the imaging of tumors, in orthotopic models. Consequently, addressing strategies to reduce uptake in these organs was not the focus of this study. Furthermore, our objective was not to detect metastases or translate the findings directly to clinical applications in patients, but to explore the imaging capabilities of the RNPs, which the results successfully support.

Conclusion

This work successfully developed RNPs through the direct labeling of Soluplus®-based micellar systems with ^{99m}Tc, demonstrating potential for diagnostic and monitoring applications in preclinical research using radioisotopic imaging, in line with the 3Rs concept in the use of experimental animals. The in vivo performance evaluation, guided by an optimized imaging protocol, yielded promising results, as [^{99m}Tc]Tc-Soluplus® enabled the visualization of tumors in murine models of breast and colon cancer via scintigraphy studies. The passive targeting approach leveraged the enhanced permeability and retention (EPR) effect, which is driven by tumor angiogenesis and results in large fenestrations in the endothelial cells of blood vessels, facilitating nanoparticle accumulation while minimizing elimination through the liver, spleen, and kidneys. Additionally, functionalizing the RNPs with glucose and bevacizumab enhanced tumor uptake and anchoring by employing active targeting strategies, which are central to the next generation of nanomaterials. This experimental design underscores the importance of further investigating the biological characteristics that determine the success of diagnostic RNPs, optimizing imaging acquisition conditions, and understanding their metabolism, dosimetry, and effects on non-target organs. These efforts will contribute to the ongoing development of innovative imaging tools for preclinical research.

Abbreviations

CMC	Critical Micellar Concentration
DLS	Dynamic Light Scattering
EPR	Enhanced Permeability and Retention
GLUT	Glucose Transporter
ITLC	Instant Thin Layer Chromatography
RNP	Radionanoprobe
SPECT	Single Photon Emission Computed Tomography
TPGS	d-α-tocopheryl polyethylene glycol succinate 1000
VEGFR	Vascular Endothelial Growth Factor Receptor

Acknowledgements
Not applicable.

Author contributions
Conceptualization – MJS; Methodology – MJS, MP, FT, MN, VM, MM, DC; Formal analysis – MJS, DC, MZ; Writing – Original Draft – MJS; Writing – Review & Editing – MJS, MP, MZ.

Funding
This project was funded by the Secretariat of Science and Technology (SeCyT) of the University of Buenos Aires (UBACyT 20020220300178BA, Res. (C.S.) 1384/23).

Data availability
The datasets generated during and/or analyzed during the current study are available from the corresponding author on reasonable request.

Declarations

Ethical approval
All procedures performed with animals are approved by the Institutional Commission for the Care and Use of Laboratory Animals (CICUAL) of the School of Pharmacy and Biochemistry, University of Buenos Aires (Res (D) N°671/18). All methods were carried out in accordance with CICUAL and ARRIVE guidelines and regulations.

Consent to participate
Not applicable.

Consent for publication
Not applicable.

Competing interests
The authors declare that they have no competing interests.

Received: 23 July 2024 / Accepted: 19 September 2024
Published online: 29 October 2024

References

Albanese A, Tang PS, Chan WC. The effect of nanoparticle size, shape, and surface chemistry on biological systems. Annu Rev Biomed Eng. 2012. https://doi.org/10.1146/annurev-bioeng-071811-150124.
Allen TM, Cullis PR. Liposomal drug delivery systems: from concept to clinical applications. Adv Drug Deliv Rev. 2013. https://doi.org/10.1016/j.addr.2012.09.037.
American Type Culture Collection. CT26.WT colon carcinoma cell line. https://www.atcc.org/products/crl-2638 (2024a). Accessed 02 Feb 2024.
American Type Culture Collection. 4T1 murine cell line. https://www.atcc.org/Products/All/CRL-2539.aspx (2024b). Accessed 02 Feb 2024.
Argentine Pharmacopeia 7th Ed. Vol. III. Monograph of Sodium Pertechnetate (99mTc) Solution for injection. In Radiopharmaceutical Products Sect. 2013. pp. 660–661. https://www.argentina.gob.ar/sites/default/files/libro_tercero.pdf. Accessed 10 Jun 2024.
Arranja A, Ivashchenko O, Denkova AG, Morawska K, van Vlierberghe S, Dubruel P, et al. SPECT/CT Imaging of Pluronic Nanocarriers with varying poly(ethylene oxide) block length and aggregation state. Mol Pharm. 2016;13(3):1158–65. https://doi.org/10.1021/acs.molpharmaceut.5b00958.
Bao A, Goins B, Klipper R, Negrete G, Mahindaratne M, Phillips WT. A novel liposome radiolabeling method using 99mTc-SNS/S complexes: in vitro and in vivo evaluation. J Pharm Sci. 2003. https://doi.org/10.1002/jps.10441.
Belhaj-Tayeb H, Briane D, Vergote J, et al. In vitro and in vivo study of ^{99m}Tc-MIBI encapsulated in PEG-liposomes: a promising radiotracer for tumour imaging. Eur J Nucl Med Mol Imaging. 2003. https://doi.org/10.1007/s00259-002-1038-4.
Boerman OC, Laverman P, Oyen WJ, Corstens FH, Storm G. Radiolabeled liposomes for scintigraphic imaging. Prog Lipid Res. 2000. https://doi.org/10.1016/s0163-7827(00)00013-8.
Briceño Fernández V, Hermida Alava K, Bernabeu E, Fuentes P, Brito Devoto T, Höcht C, et al. Highly effective inhalable voriconazole-loaded nanomicelles for fungal infections in cystic fibrosis patients: a promising therapeutic strategy for allergic bronchopulmonary aspergillosis. J Drug Deliv Sci Technol. 2024;100(106126). https://doi.org/10.1016/j.jddst.2024.106126.
Carmo VA, Ferrari CS, Reis EC, Ramaldes GA, Pereira MA, De Oliveira MC, et al. Biodistribution study and identification of inflammation sites using 99mTc-labelled stealth pH-sensitive liposomes. Nucl Med Commun. 2008. https://doi.org/10.1097/MNM.0b013e3282f1bc0d.
Dams ET, Oyen WJ, Boerman OC, Storm G, Laverman P, Koenders EB, et al. Technetium-99m-labeled liposomes to image experimental colitis in rabbits: comparison with technetium-99m-HMPAO-granulocytes and technetium-99m-HYNIC-IgG. J Nucl Med. 1998;39(12):2172–8.
Deshmukh AS, Chauhan PN, Noolvi MN, Chaturvedi K, Ganguly K, Shukla SS, et al. Polymeric micelles: basic research to clinical practice. Int J Pharm. 2017. https://doi.org/10.1016/j.ijpharm.2017.09.005.
Dian L, Yu E, Chen X et al. Enhancing oral bioavailability of quercetin using novel soluplus polymeric micelles. Nanoscale Res Lett 2014 9, 684. https://doi.org/10.1186/1556-276X-9-684
Djuric D, Hardung H. Soluplus - the solid solution. ExAct. 2009;23:2–5.
Fuentes P, Bernabeu E, Bertera F, Garces M, Oppezzo J, Zubillaga M, et al. Dual strategy to improve the oral bioavailability of efavirenz employing nanomicelles and curcumin as a bio-enhancer. Int J Pharm. 2024;651:123734. https://doi.org/10.1016/j.ijpharm.2023.123734.
Galdopórpora JM, Martinena C, Bernabeu E, Riedel J, Palmas L, Castangia I, et al. Inhalable Mannosylated rifampicin–curcumin co-loaded nanomicelles with enhanced in Vitro Antimicrobial efficacy for an optimized pulmonary tuberculosis therapy. Pharmaceutics. 2022;14(5):959. https://doi.org/10.3390/pharmaceutics14050959.
Ganapathy V, Thangaraju M, Prasad P. Nutrient transporters in cancer: relevance to Warburg hypothesis and beyond. Pharmacol Ther. 2009. https://doi.org/10.1016/j.pharmthera.2008.09.005.
Girón D, Gómez GE, Casal JJ, Delfino JM, Gomez F, Ibarra C, et al. Soluplus® nanomicelles enhance IgG neutralizing properties against Shiga toxin type 2. J Drug Deliv Sci Technol. 2024;95:105606. https://doi.org/10.1016/j.jddst.2024.105606.

Grotz E, Tateosian NL, Salgueiro J, Bernabeu E, Gonzalez L, Manca ML, et al. Pulmonary delivery of rifampicin-loaded soluplus micelles against Mycobacterium tuberculosis. J Drug Deliv Sci Technol. 2019;53(101170). https://doi.org/10.1016/j.jddst.2019.101170.

Hardung H, Djuric D, Shaukat A, Combining. HME & solubilization: Soluplus® - the solid solution. Drug Del Tech. 2010;10:20–7.

Instituto Nacional del Cáncer. Estadísticas – Incidencia. https://www.argentina.gob.ar/salud/instituto-nacional-del-cancer/estadisticas/incidencia (2020). Accessed 19 Jun 2024.

Jin X, Zhou B, Xue L, San W. Soluplus® micelles as a potential drug delivery system for reversal of resistant tumor. Biomed Pharmacother. 2015;69:388–95. https://doi.org/10.1016/j.biopha.2014.12.028.

Kizjakina K, Bryson J, Grandinetti G, Reineke T. Cationic glycopolymers for the delivery of pDNA to human dermal fibroblasts and rat mesenchymal stem cells. Biomaterials. 2012. https://doi.org/10.1016/j.biomaterials.2011.10.031.

Li X, Zhou H, Yang L, Du G, Pai-Panandiker A, Huang X, et al. Enhancement of cell recognition in vitro by dual-ligand cancer targeting gold nanoparticles. Biomaterials. 2011. https://doi.org/10.1016/j.biomaterials.2010.12.031.

Longmire M, Choyke PL, Kobayashi H. Clearance properties of nano-sized particles and molecules as imaging agents: considerations and caveats. Nanomed (Lond). 2008. https://doi.org/10.2217/17435889.3.5.703.

Maeda H, Wu J, Sawa T, Matsumura Y, Hori K. Tumor vascular permeability and the EPR effect in macromolecular therapeutics: a review. J Control Release. 2000. https://doi.org/10.1016/s0168-3659(99)00248-5.

Maravajjala KS, Swetha KL, Sharma S, Padhye T, Roy A. Development of a size-tunable paclitaxel micelle using a microfluidic-based system and evaluation of its in-vitro efficacy and intracellular delivery. J Drug Deliv Sci Technol. 2020;60:102041. https://doi.org/10.1016/j.jddst.2020.102041.

Medina RA, Owen GI. Glucose transporters: expression, regulation and cancer. Biol Res. 2002;35(1):9–26.

Moretton MA, Cagel M, Bernabeu E, Gonzalez L, Chiappetta DA. Nanopolymersomes as potential carriers for rifampicin pulmonary delivery. Colloids Surf B Biointerfaces. 2015. https://doi.org/10.1016/j.colsurfb.2015.10.049.

Moretton MA, Bernabeu E, Grotz E, Gonzalez L, Zubillaga M, Chiappetta DA. A glucose-targeted mixed micellar formulation outperforms Genexol in breast cancer cells. Eur J Pharm Biopharm. 2017;114:305–16. https://doi.org/10.1016/j.ejpb.2017.02.005.

Mosleh-Shirazi S, Abbasi M, Shafiee M, Kasaee SR, Amani AM. Renal clearable nanoparticles: an expanding horizon for improving biomedical imaging and cancer therapy. Mater Today Commun. 2021;26:102064. https://doi.org/10.1016/j.mtcomm.2021.102064.

Mueckler M, Thorens B. The SLC2 (GLUT) family of membrane transporters. Mol Aspects Med. 2013. https://doi.org/10.1016/j.mam.2012.07.001.

National Research Council (US). Committee for the update of the guide for the Care and Use of Laboratory animals. Guide for the Care and Use of Laboratory animals. 8th ed. Washington (DC): National Academies Press (US); 2011.

Nichols JW, Bae YH. EPR: evidence and fallacy. J Control Release. 2014. https://doi.org/10.1016/j.jconrel.2014.03.057.

Nicoud MB, Ospital IA, Táquez Delgado MA, Riedel J, Fuentes P, Bernabeu E, et al. Nanomicellar formulations loaded with histamine and paclitaxel as a New Strategy to improve chemotherapy for breast Cancer. Int J Mol Sci. 2023;24(4):3546. https://doi.org/10.3390/ijms24043546.

Niu J, Wang A, Ke Z, Zheng Z. Glucose transporter and folic acid receptor-mediated Pluronic P105 polymeric micelles loaded with doxorubicin for brain tumor treating. J Drug Target. 2014. https://doi.org/10.3109/1061186X.2014.913052.

Owen SC, Chan DPY, Shoichet MS. Polymeric micelle stability. Nano Today. 2012. https://doi.org/10.1016/j.nantod.2012.01.002.

Pereira MA, Mosqueira VC, Carmo VA, Ferrari CS, Reis EC, Ramaldes GA, et al. Biodistribution study and identification of inflammatory sites using nanocapsules labeled with (99m)Tc-HMPAO. Nucl Med Commun. 2009. https://doi.org/10.1097/MNM.0b013e32832f2b59.

Psimadas D, Bouziotis P, Georgoulias P, Valotassiou V, Tsotakos T, Loudos G. Radiolabeling approaches of nanoparticles with 99mTc. Contrast Media Mol Imaging. 2013;8:333–9. https://doi.org/10.1002/cmmi.1530.

Psimadas D, Oliveira H, Thevenot J, Lecommandoux S, Bouziotis P, Varvarigou AD, et al. Polymeric micelles and vesicles: biological behavior evaluation using radiolabeling techniques. Pharm Dev Technol. 2014. https://doi.org/10.3109/10837450.2013.763264.

Ramos-Membrive R, Erhard A, Luis de Redín I, Quincoces G, Collantes M, Ecay M, et al. In vivo SPECT-CT imaging and characterization of technetium-99m-labeled bevacizumab-loaded human serum albumin pegylated nanoparticles. J Drug Deliv Sci Technol. 2021;64:101809. https://doi.org/10.1016/j.jddst.2020.101809.

Riedel J, Calienni MN, Bernabeu E, Calabro V, Lázaro-Martinez JM, Prieto MJ, et al. Paclitaxel and Curcumin co-loaded mixed micelles: improving in vitro efficacy and reducing toxicity against Abraxane®. J Drug Deliv Sci Technol. 2021;62:102343. https://doi.org/10.1016/j.jddst.2021.102343.

Riedel J, Pibuel M, Bernabeu E, Poodts D, Díaz M, Allo M, et al. Glycosylated paclitaxel mixed nanomicelles: increasing drug brain accumulation and enhancing its in vitro antitumoral activity in glioblastoma cell lines. J Drug Deliv Sci Technol. 2022;68:103046. https://doi.org/10.1016/j.jddst.2021.103046.

Sawant RR, Torchilin VP. Challenges in development of targeted liposomal therapeutics. AAPS J. 2012. https://doi.org/10.1208/s12248-012-9330-0.

Seo H, Nam S, Im HJ, et al. Rapid Hepatobiliary Excretion of Micelle-Encapsulated/Radiolabeled Upconverting Nanoparticles as an Integrated Form. Sci Rep. 2015;5:15685. https://doi.org/10.1038/srep15685.

Song E, Manganiello M, Chow Y, Ghosn B, Convertine A, Stayton P, et al. In vivo targeting of alveolar macrophages via RAFT-based glycopolymers. Biomaterials. 2012. https://doi.org/10.1016/j.biomaterials.2012.06.025.

Szablewski L. Expression of glucose transporters in cancers. Biochim Biophys Acta. 2013. https://doi.org/10.1016/j.bbcan.2012.12.004.

Taich P, Moretton MA, Del Sole MJ, Winter U, Bernabeu E, Croxatto JO, et al. Sustained-release hydrogels of topotecan for retinoblastoma. Colloids Surf B Biointerfaces. 2016. https://doi.org/10.1016/j.colsurfb.2016.07.001.

Tesan FC, Portillo MG, Moretton MA, Bernabeu E, Chiappetta DA, Salgueiro MJ, et al. Radiolabeling and biological characterization of TPGS-based nanomicelles by means of small animal imaging. Nucl Med Biol. 2017. https://doi.org/10.1016/j.nucmedbio.2016.09.006.

Tesán FC, Cerqueira-Coutinho C, Salgueiro MJ, de Souza Albernaz M, Rocha Pintos S, Rezende Dos Reis SR, et al. Characterization and biodistribution of Bevacizumab TPGS-based nanomicelles: preliminary studies. J Drug Deliv Sci Technol. 2016;36:95–8. https://doi.org/10.1016/j.jddst.2016.09.011.

Tesán F, Portillo M, Giaquinta D, Nicoud M, Moretton M, Zubillaga M, et al. TPGS based 99mTc nano radiopharmaceuticals: potential application in breast cancer diagnosis. Medicina. 2018;78(Suppl III):196.
Torchilin VP. Lipid-core micelles for targeted drug delivery. Curr Drug Deliv. 2005. https://doi.org/10.2174/156720105774370221.
Torchilin VP, Nanocarriers. Pharm Res. 2007a. https://doi.org/10.1007/s11095-007-9463-5.
Torchilin VP. Targeted pharmaceutical nanocarriers for cancer therapy and imaging. AAPS J. 2007b. https://doi.org/10.1208/aapsj0902015.
Underwood C, van Eps AW, Ross MW, Laverman P, van Bloois L, Storm G, et al. Intravenous technetium-99m labelled PEG-liposomes in horses: a safety and biodistribution study. Equine Vet J. 2012. https://doi.org/10.1111/j.2042-3306.2011.00403.x.
Wang Y, Grayson SM. Approaches for the preparation of non-linear amphiphilic polymers and their applications to drug delivery. Adv Drug Deliv Rev. 2012. https://doi.org/10.1016/j.addr.2012.03.011.
Wang Y, Zhang X, Yu P, Li C. Glycopolymer micelles with reducible ionic cores for hepatocytes-targeting delivery of DOX. Int J Pharm. 2013. https://doi.org/10.1016/j.ijpharm.2012.12.001.
Wegmann M, Parola L, Bertera FM, Taira CA, Cagel M, Buontempo F, et al. Novel carvedilol paediatric nanomicelle formulation: in-vitro characterization and in-vivo evaluation. J Pharm Pharmacol. 2017;69(5):544–53. https://doi.org/10.1111/jphp.12605.
Ying X, Wen H, Lu W, Du J, Guo J, Tian W, et al. Dual-targeting daunorubicin liposomes improve the therapeutic efficacy of brain glioma in animals. J Control Release. 2010. https://doi.org/10.1016/j.jconrel.2009.09.020.
Zhu GH, Gray ABC, Patra HK. Nanomedicine: controlling nanoparticle clearance for translational success. Trends Pharmacol Sci. 2022;43(9):709–11. https://doi.org/10.1016/j.tips.2022.05.001.

Publisher's note

Springer Nature remains neutral with regard to jurisdictional claims in published maps and institutional affiliations.